CHAOS
Theory and Applications
in Applied Sciences and Engineering

e-ISSN: 2687-4539
RESEARCH ARTICLE
Vol.7 / No.1 / 2025 / pp.1-9
https://doi.org/10.51537/chaos.1518307

Demonstration of Sensitive Analysis and Optical Soliton Patterns in a (4+1) Dimensional Boiti-Leon-Manna Pempinelli Equation: Dynamic Insights into Bifurcation, Chaotic Behavior

Muhammad Iqbal [*,1], **Muhammad Bilal Riaz** [α,β,2], **Muhammad Aziz ur Rehman** [*,3], **Tomas Martinovic** [α,4] **and Jan Martinovic** [α,5]

*Department of Mathematics, University of Management and Technology, Lahore, Pakistan, [α]IT4Innovations, VSB – Technical University of Ostrava, Ostrava, Czech Republic, [β]Department of Computer Science and Mathematics, Lebanese American University,, Byblos, Lebanon.

ABSTRACT This study aims to find exact solutions for a mathematical problem known as the (4+1)-dimensional Boiti Leon Manna Pempinelli (BLMP) equation. In order to convert the governing equation into an ordinary differential equation, we make use of an appropriate wave transformation. This transformation enables the investigation of mathematical solutions, exaggerated outcomes, and normal solutions. Furthermore, in order to accurately determine the solution to this wave, we make use of the modified Khater method. We apply the given approach to find rational, the trigonometric, and hyperbolic solutions. The selected solutions provide graphic representations that accurately depict the physical behavior of the model. Using their visualization, we are able to demonstrate how their behavior changes over time in a four-dimensional space. The use of a visual representation, which involves selecting suitable values for arbitrary components, improves the understanding of the dynamical system. Furthermore, we conduct a sensitivity analysis of the dynamical system to determine the stability of the solution. The dynamical system engages in a discussion about the existence of chaotic dynamics within the Boiti Leon Manna Pempinelli equation. It is possible to depict these chaotic phenomena using two-dimensional and three-dimensional phase portraits.

KEYWORDS
Boiti Leon Manna Pempinelli equation
Modified Khater method
Dynamical system
Solitary wave analysis
Exact solutions

INTRODUCTION

For the purpose of expressing the issues that arise in nonlinear phenomena, we use the nonlinear partial differential equation (PDE). These phenomena include hydrodynamics, plasma physics, chemical dynamics, photobiology, solid physics, marine and atmospheric phenomena, and many more. As a result of these disciplines, it is clear that the traveling wave solutions of nonlinear evolution equations play a significant part in the investigation. For the purpose of finding exact solutions to nonlinear partial differential equations (PDEs), explorers provided the following of these methods, such as the first integral method (Feng 2002), Jacobi elliptic function expansion method (Liu *et al.* 2001), F- expansion method (Sheng 2006), exp-function method (He and Zhang 2008), the Kudryashov method (Kim *et al.* 2014), the improved$(\frac{G'}{G})$-expansion method (Wu *et al.* 2023), the tanh-coth method(Wazwaz 2007), tanh-sech method (Ma 1993), projective Riccati equation method(Conte and Musette 1992), Kudryashov method (Kudryashov 1991), sine-cosine method (Wazwaz 2004), Hirota bilinear method (Wang 2009), bifurcation theory method of dynamic systems(Li *et al.* 2015). Valdés et al present a historical-problemic focus of a course of ordinary differential equations (Valdés 2003).

In recent times, the nonlinear evolution equations have been making significant contributions to the accomplishment of several scientific goals in a variety of domains(Khater 2021b). It was

Manuscript received: 4 July 2024,
Revised: 28 September 2024,
Accepted: 7 October 2024.

[1]iqbalakhtar167@gmail.com.pk(**Corresponding author**)
[2]muhammad.bilal.riaz@vsb.cz
[3]aziz.rehman@umt.edu.pk
[4]Tomas.martinovic@vsb.cz
[5]Jan.martinovic@vsb.cz

John Scott Russell's discovery of the soliton wave that marked the beginning of this progression (Tchaho *et al.* 2021). The characteristics of this particular form of wave have piqued the interest of several scientists from various fields, leading to the discovery of some of these characteristics (Khater 2021a). In 1965, Zabusky and Kruskal discovered the soliton wave language, which followed the photon, proton, and other particles. After an interaction, Soliton is a restricted framework that maintains control over its identity (Al-Smadi *et al.* 2021). Solitary waves are used to describe the propagation of undulation pulses or packets in nonlinear dispersive media(Kruglov and Triki 2021). It is because of the dynamical balance between the nonlinear effects and the dispersive effects that these undulations keep their stable structure(Nikan *et al.* 2021).

A soliton is an uncommon individual undulation that maintains its soliton structure regardless of whether or not it comes into contact with other solitons (Al-Smadi 2018). That seemingly insignificant factor exerts a substantial influence on scientific thought (Khater *et al.* 2021c). All of these findings have led a significant number of mathematicians to perceive themselves as important contributors to development. This is not limited to mathematics or any one field of study, rather it encompasses their participation in the development of all scientific breakthroughs, as well as the expansion of society and mankind(Akinyemi *et al.* 2021).

Researchers from all around the world have been interested in higher-dimensional NLEEs. Researchers have discovered a broad variety of solutions for NLEEs in higher dimensions, including quasiperiodic, rogue wave, and lump wave solutions (Fokas 2016). Recent research has hypothesized the existence of integrable NLEE models that have three or more spatial dimensions (Xu and Huang 2013). The Lax Pair extension allows for the derivation of the (4 + 1)-dimensional Fokas equation (Zheng-Zheng and Zhen-Ya 2009) from the Kadomtsev-Petviashvili (KP) equation in the (2 + 1)-dimensional space. This equation has been a part of extensive research, which has included findings on issues such as point symmetry, potential symmetry, rogue waves, multisolitons, and a great deal more (Lee *et al.* 2010). The fact that there exist a substantial number of higher-dimensional models, such as those suggested by (Xu and Wazwaz 2019), offers us a source of inspiration.

One of the most efficient methods for finding the exact solution of NLEEs is the modified Khater technique (Biswas *et al.* 2016) were the ones who first developed it, and many publications in the past considered it to be a modified auxiliary equation approach. Due to its simplicity and consistency, it can reduce computing labor, indicating its wide range of use. This technique, which relies on the auxiliary equation, benefits from seven strategies. This strategy is beneficial as it eliminates the need for precise solutions to numerous integer and fractional-order nonlinear PDEs. One further use of it is to provide evidence that a set of solutions does in fact exist (Singh *et al.* 2018). A lot of people have used this method to find single-wave solutions to nonlinear partial differential equations (PDEs). Some examples are the fractional order Sharma Tasso-Olever (STO) equation(Bibi *et al.* 2017), the Bogoyavlenskii equations system (Khater *et al.* 2017), the fractional emerging telecommunication model (Park *et al.* 2020), and the nonlinear Schrodinger equation (Khater *et al.* 2021a).

Khater *et al.* (2021a), recently conducted an analysis of a variety of physical phenomena obtained numerical and analytical solutions. Some of these answers were the Gilson Pickering equation, nonlinear wave packets, ultrashort optical solitons, the Caudrey-Dodd Gibbon equation, ultra-short pulse phase shifts, and the Chen Lee Liu equation that has been changed. In this article, we use the modified Khater technique to examine the Boiti-Leon-Manna Pempinelli Equation, which is a four-dimensional equation, in order to find closed form solitary wave solutions and solitons. This investigation was motivated by prior research studies.

The use of bifurcation analysis to differential equations has emerged as an intriguing topic of study in recent years (Liu *et al.* 2022). Using a cascaded system, Raza *et al.* (2024) investigated wave phenomena that were quasiperiodic, periodic, and super nonlinear. Saha (2017) find the bifurcation, periodic and chaotic motions of the modified equal width-Burgers (MEW-Burgers) equation with external periodic perturbation in nonlinear dynamics. Many researchers have used bifurcation analysis to investigate both the disturbed and unperturbed nature of dynamical systems. Jamal and others established soliton solutions of the nerve impulse model (Jamal *et al.* 2023). They utilized the theory of bifurcation and chaos to understand the multistability, sensitivity analysis, chaos, and bifurcation of the nerve impulse model, as well as the concept of external disturbance. They use bifurcation to determine equilibrium points and calculate all phase portraits of a dynamical system. To clarify whether the model under discussion is chaotic or not, chaos theory provides the answer. Specifically, it suggests that when we apply an external force to the solutions to physical events that occur in nonlinear media, the solutions either remain stable or become chaotic.

The beginning circumstances solely determine the behavior of autonomous dynamical systems at the asymptotic level. In the realm of equilibrium behaviors, there are four distinct types: a limit circle, a tour, an equilibrium point, and chaos. This study centers on chaos theory to investigate the dynamical system under discussion. There are many different approaches to assessing whether or not chaos exists. This current research highlights the most advantageous ones. Lyapounov exponents, phase portraits, time series, Poincaré maps, bifurcation diagrams, and power spectrums are some of the most prominent approaches, as stated by (Özer and Akın 2005). Various techniques, such as the Lyapunov dimension, the correlation dimension, and entropy, can identify chaos. However, the difficulty of identifying chaos in real-world systems often discourages the use of these techniques.

This article is organized into the following sections: In Section 2, the equation that governs the system is given, along with a review of the modified Khater method that was used. In Section 3, a graphical depiction of the solutions that were achieved is shown. The investigation of bifurcation analysis is encompassed within the section denoted by 4. A demonstration of chaos theory and sensitivity analysis is present in section 5. In the section referred to as 6, an explanation of the conclusion is provided.

GOVERNING EQUATION

This study uses the Boiti Leon Manna Pempinelli (BLMP) equation with(4+1)-dimensions (Raza *et al.* 2022) to discuss the movement of a compressible fluid in a structure.

$$\begin{aligned} h_{yt} + h_{zt} + h_{st} + a_1 h_{xxxy} + a_1 h_{xxxz} + a_1 h_{xxxs} + \\ a_2 h_x (h_{xy} + h_{xz} + h_{xs}) + a_2 h_{xx} (h_y + h_z + h_s) = 0. \end{aligned} \tag{1}$$

Here, t represents time, whereas x, y, z, and s represent the dimensions of space. Furthermore, we use the symbols a_1 and a_2 to represent real constants that are not zero and have an arbitrary nature. Eq.(2) is derived from the Boiti-Leon-Manna-Pempinelli (BLMP) equation, which has four dimensions. To investigate the system summarized by Eq. (1), using specific wave transformation that is,

$$h(x, y, z, s, t) = f(\xi).$$

Where, $\xi = k_1x + k_2y + k_3z + k_4s - ct$, k denotes the wave width and c represents the wave speed. By utilizing wave transformation we finally have,

$$\delta_0 f'' + \delta_1 f'''' + \delta_2 f' f'' = 0. \tag{2}$$

Integrating Eq. (2), we have the equation

$$\delta_0 f' + \delta_1 f''' + \delta_2 \frac{(f')^2}{2} = 0. \tag{3}$$

Let $\frac{\delta_2}{2} = \delta_2^*$, we have

$$\delta_0 f' + \delta_1 f''' + \delta_2^* (f')^2 = 0. \tag{4}$$

Execution of Modified Khater Method

In this part of article, the method provided by (Khater *et al.* 2021b) is used to extract the solitary wave solutions of the equation that is being discussed. We can view the plots of the discussed results by selecting proper values for the parameters.

Step(1): Following is a statement that illustrates the general structure of a nonlinear partial differential equation.

$$G(h, h_x, h_{xx}, ..., h_y, h_{yy}, ..., h_z, h_{zz}, ..., h_s, h_{ss}, ..., h_t, h_{tt}, ...) = 0. \tag{5}$$

In this context, the expression h = $h(x, y, z, s, t)$ is not familiar, and G is a representation of a polynomial function with regard to certain variables ξ.

Step(2):The transformation has been used in the following way:

$$h(x, y, z, s, t) = f(\xi), \;\; \xi = k_1x + k_2y + k_3z + k_4s - ct,$$

by converting this into simple form as:

$$G(f, f', f'', f''', ...) = 0,$$

the prime number f denotes the derivative with respect to ξ.

Step (3): A possible initial solution to the above equation is as follows

$$f(\xi) = \sum_{j=0}^{n} \Lambda_j \Omega^j(\xi). \tag{6}$$

For each $\Lambda_j (0 \le j \le n)$, the constants are chosen at random, and $\Omega(\xi)$ represents the solution to the equation that is required.

$$f(\xi) = \Lambda_0 + \Lambda_1 \Omega(\xi). \tag{7}$$

The general solution to nonlinear ordinary differential equations may be written as:

$$\Omega'(\xi) = a_1 ln(v) + a_2\, \Omega(\xi) \ln(v) + a_3\, \Omega^2(\xi)\, ln(v). \tag{8}$$

Here, a_1, a_2 *and* a_3 are real constants.

Step(4): The highest order derivative f''' and the highest order nonlinear term $(f')^2$ in Eq.5 are balanced to get n=1 in accordance with the homogeneous balance principle.

Step(5):The following set of algebraic equations is constructed using Eq.8 and Eq.9 in Eq.7,and they are balanced to zero by the coefficients of each power of Ω.

$$\begin{cases}
\Omega^{0J}(\xi) & : \Lambda_1^2\, a_1^2\, ln(v)^2 \mu + \Lambda_1\, a_1\, ln(v)\, \lambda + \Lambda_1 (2\Delta a_1^2\, ln(v)^3 \\
& + a\, ln(v)^3\, a_2^2) = 0, \\
\Omega^{1J}(\xi) & : 2\Lambda_1^2\, a_1\, ln(v)^2\, a_2\, \mu + \Lambda_1\, ln(v)\, a_2 \lambda + \Lambda_1 (a_2 (2a_1\, ln(v)^2 \Delta \\
& + ln(v)^2 a_2^2) ln(v) + 6\Delta\, a_2\, ln(v)^3) a_1 = 0, \\
\Omega^{2J}(\xi) & : \Lambda_1^2 (2a_1\, ln(v)^2\, \Delta + ln(v)^2\, a_2^2) \mu + \Lambda_1\, \Delta\, ln(v)\, \lambda + \\
& \Lambda_1 (3a_2^2\, ln(v)^3\, \Delta + (4\Delta (2a_1\, ln(v)^2\, \Delta + ln(v)^2\, a_2^2) ln(v)) \sigma = 0, \\
\Omega^{3J}(\xi) & : 12\Lambda_1\, a_2\, \Delta^2\, ln(v)^3\, \sigma + 2\Lambda_1^2\, ln(v)^2\, a_2\, \Delta\, \mu = 0, \\
\Omega^{4J}(\xi) & : 6\Lambda_1\, \Delta^3\, ln(v)^3\, \sigma + \Lambda_1^2\, \Delta^2\, ln(v)^2\, \mu = 0.
\end{cases}$$

Solving the system of algebraic equations with the assistance of Maple allows for the acquisition of distinct solution sets. With the help of the Eq.5, we are able to get the following exact solutions.

$$\Lambda_0 = \Lambda_0,\; \Lambda_1 = -\frac{6a_3\lambda}{ln(v)(4a_3a_1 - a_2^2)\mu}.$$

We used the obtained values of the parameters to determine the solitary wave of Eq.(1), which led to the following results as:

Case1: If $\Delta = a_2^2 - 4a_1a_3 < 0$ and $a_3 \neq 0$,

$$\begin{cases}
h_1(x,y,z,s,t) & = \frac{(\ln(v)\mu)\left(4\,a_1a_3 - a_2^2\right) + 3\sqrt{-\Delta}\tan_v(\frac{1}{2}\sqrt{-\Delta}\xi)\lambda - 3\lambda a_2}{\mu ln(v)(4a_1a_3 - a_2^2)}, \\
h_2(x,y,z,s,t) & = -\frac{(\ln(v)\mu)\left(4\,a_1a_3 - a_2^2\right) + 3\sqrt{-\Delta}\cot_v(\frac{1}{2}\sqrt{-\Delta}\xi)\lambda}{\mu ln(v)(4a_1a_3 - a_2^2)} \\
& + \frac{3\lambda a_2}{\mu ln(v)(4a_1a_3 - a_2^2)}, \\
h_3(x,y,z,s,t) & = \frac{(\ln(v)\mu)\left(4\,a_1a_3 - a_2^2\right) - 3\sqrt{-\Delta}\sqrt{rs}\sec_v\left(\sqrt{-\Delta}\xi\right)\lambda}{\mu\, \ln(v)(4\,a_1a_3 - a_2^2)} \\
& - \frac{3\sqrt{-\Delta}\tan_v\left(\sqrt{-\Delta}\xi\right)\lambda + 3\,\lambda\, a_2}{\mu\, \ln(v)(4\,a_1a_3 - a_2^2)}, \\
h_4(x,y,z,s,t) & = \frac{(\ln(v)\mu)\left(4\,a_1a_3 - a_2^2\right) - 3\sqrt{-\Delta}\csc_v\left(\sqrt{-\Delta}\xi\right)\sqrt{rs}\lambda}{\mu\, \ln(v)(4\,a_1a_3 - a_2^2)} \\
& - \frac{3\sqrt{-\Delta}\cot_v\left(\sqrt{-\Delta}\xi\right)\lambda + 3\,\lambda\, a_2}{\mu\, \ln(v)(4\,a_1a_3 - a_2^2)}, \\
h_5(x,y,z,s,t) & = \frac{(2\ln(v)\mu)\left(4\,a_1a_3 - a_2^2\right) - 3\sqrt{-\Delta}\tan_v\left(\frac{1}{4}\sqrt{-\Delta}\xi\right)\lambda}{2\mu\, \ln(v)(4\,a_1a_3 - a_2^2)} \\
& + \frac{3\sqrt{-\Delta}\cot_v\left(\frac{1}{4}\sqrt{-\Delta}\xi\right)\lambda + 6\,\lambda\, a_2}{2\mu\, \ln(v)(4\,a_1a_3 - a_2^2)}.
\end{cases} \tag{9}$$

Case 2: If $\Delta = a_2^2 - 4a_1a_3 > 0$ *and* $a_3 \neq 0$,

$$\begin{cases}
h_6(x,y,z,s,t) & = \frac{(\ln(v)\mu)\left(4\,a_1a_3 - a_2^2\right) + 3\,\tanh_v\left(\frac{1}{2}\sqrt{\Delta}\xi\right)\sqrt{\Delta}\lambda}{\mu\, \ln(v)(4\,a_1a_3 - a_2^2)} \\
& + \frac{3\,\lambda\, a_2}{\mu\, \ln(v)(4\,a_1a_3 - a_2^2)}, \\
h_7(x,y,z,s,t) & = \frac{(\ln(v)\mu)\left(4\,a_1a_3 - a_2^2\right) + 3\,\coth_v\left(\frac{1}{2}\sqrt{\Delta}\xi\right)\sqrt{\Delta}\lambda}{\mu\, \ln(v)(4\,a_1a_3 - a_2^2)} \\
& + \frac{3\,\lambda\, a_2}{\mu\, \ln(v)(4\,a_1a_3 - a_2^2)}, \\
h_8(x,y,z,s,t) & = \frac{(\ln(v)\mu)\left(4\,a_1a_3 - a_2^2\right) + 3\sqrt{\Delta}\sqrt{rs}\,\mathrm{sech}_v\left(\sqrt{\Delta}\xi\right)\iota\lambda}{\mu\, \ln(v)(4\,a_1a_3 - a_2^2)} \\
& + \frac{3\sqrt{\Delta}\tanh_v\left(\sqrt{\Delta}\xi\right)\lambda + 3\,\lambda\, a_2}{\mu\, \ln(v)(4\,a_1a_3 - a_2^2)}, \\
h_9(x,y,z,s,t) & = \frac{(\ln(v)\mu)\left(4\,a_1a_3 - a_2^2\right) + 3\sqrt{\Delta}\; cosech_v\left(\sqrt{\Delta}\xi\right)\sqrt{rs}\lambda}{\mu\, \ln(v)(4\,a_1a_3 - a_2^2)} \\
& + \frac{3\sqrt{\Delta}\coth_v\left(\sqrt{\Delta}\xi\right)\lambda + 3\,\lambda\, a_2}{\mu\, \ln(v)(4\,a_1a_3 - a_2^2)}, \\
h_{10}(x,y,z,s,t) & = \frac{(2\ln(v)\mu)\left(4\,a_1a_3 - a_2^2\right) + 3\,\tanh_v\left(\frac{1}{4}\sqrt{\Delta}\xi\right)\sqrt{\Delta}\lambda}{2\mu\, \ln(v)(4\,a_1a_3 - a_2^2)} \\
& + \frac{3\,\coth_v\left(\frac{1}{4}\sqrt{\Delta}\xi\right)\sqrt{\Delta}\lambda + 6\,\lambda\, a_2}{2\mu\, \ln(v)(4\,a_1a_3 - a_2^2)}.
\end{cases} \tag{10}$$

Case 3: If $a_3a_1 > 0$ *and* $a_2 = 0$,

$$\begin{cases} h_{11}(x,y,z,s,t) &= \frac{\left(4\ln(v)\mu a_1a_3 - \ln(v)\mu {a_2}^2\right)}{\mu\ln(v)(4a_1a_3-a_2^2)} \\ &\quad - \frac{\left(6a_3\lambda\sqrt{\frac{a_1}{a_3}}\tan_v(\sqrt{a_1a_3}\xi)\right)}{\mu\ln(v)(4a_1a_3-a_2^2)}, \\ h_{12}(x,y,z,s,t) &= \frac{\left(6a_3\lambda\sqrt{\frac{a_1}{a_3}}\cot_v(\sqrt{a_1a_3}\xi)+4\ln(v)\mu a_1a_3\right)}{\mu\ln(v)(4a_1a_3-a_2^2)} \\ &\quad - \frac{\left(\ln(v)\mu {a_2}^2\right)}{\mu\ln(v)(4a_1a_3-a_2^2)}, \\ h_{13}(x,y,z,s,t) &= \frac{\left(6\sqrt{rs}\sec_v(2\sqrt{a_1a_3}\xi)\sqrt{\frac{a_1}{a_3}}\lambda a_3\right)}{\mu\ln(v)(4a_1a_3-a_2^2)} \\ &\quad + \frac{\left(6\tan_v(2\sqrt{a_1a_3}\xi)\sqrt{\frac{a_1}{a_3}}\lambda a_3\right)}{\mu\ln(v)(4a_1a_3-a_2^2)} \\ &\quad + \frac{\left(4\ln(v)\mu a_1a_3 - \ln(v)\mu {a_2}^2\right)}{\mu\ln(v)(4a_1a_3-a_2^2)}, \\ h_{14}(x,y,z,s,t) &= \frac{\left(-6\sqrt{rs}\ cosec_v(2\sqrt{a_1a_3}\xi)\sqrt{\frac{a_1}{a_3}}\lambda a_3\right)}{\mu\ln(v)(4a_1a_3-a_2^2)} \\ &\quad + \frac{\left(6\cot_v(2\sqrt{a_1a_3}\xi)\sqrt{\frac{a_1}{a_3}}\lambda a_3\right)}{\mu\ln(v)(4a_1a_3-a_2^2)} \\ &\quad + \frac{\left(4\ln(v)\mu a_1a_3 - \ln(v)\mu {a_2}^2\right)}{\mu\ln(v)(4a_1a_3-a_2^2)}, \\ h_{15}(x,y,z,s,t) &= \frac{\left(-3\sqrt{\frac{a_1}{a_3}}\lambda a_3\right)\left(\tan\left(\frac{1}{2}\sqrt{a_1a_3}\xi\right) - \cot\left(\frac{1}{2}\sqrt{a_1a_3}\xi\right)\right)}{\mu\ln(v)(4a_1a_3-a_2^2)} \\ &\quad + \frac{\left(4\ln(v)\mu a_1a_3 - \ln(v)\mu {a_2}^2\right)}{\mu\ln(v)(4a_1a_3-a_2^2)}. \end{cases} \tag{11}$$

Case 4: If $a_3a_1 < 0$ *and* $a_2 = 0$,

$$\begin{cases} h_{16}(x,y,z,s,t) &= \frac{\left(4\ln(v)\mu a_1a_3 - \ln(v)\mu {a_2}^2\right)}{\mu\ln(v)(4a_1a_3-a_2^2)} \\ &\quad + \frac{\left(6a_3\lambda\sqrt{-\frac{a_1}{a_3}}\tanh(\sqrt{-a_1a_3}\xi)\right)}{\mu\ln(v)(4a_1a_3-a_2^2)}, \\ h_{17}(x,y,z,s,t) &= \frac{\left(6a_3\lambda\sqrt{-\frac{a_1}{a_3}}\coth(\sqrt{-a_1a_3}\xi)+4\ln(v)\mu a_1a_3\right)}{\mu\ln(v)(4a_1a_3-a_2^2)} \\ &\quad - \frac{\left(\ln(v)\mu {a_2}^2\right)}{\mu\ln(v)(4a_1a_3-a_2^2)}, \\ h_{18}(x,y,z,s,t) &= \frac{(6\sqrt{rs}\ sech_v(2\sqrt{-a_1a_3}\xi)\sqrt{-\frac{a_1}{a_3}}\ \iota\lambda a_3)}{\mu\ ln(v)(4a_1a_3-a_2^2)} \\ &\quad + \frac{(6\ tanh_v(2\sqrt{-a_1a_3}\xi)\sqrt{-\frac{a_1}{a_3}}\lambda a_3 + 4ln(v)\mu a_2^2)}{\mu\ ln(v)(4a_1a_3-a_2^2)}, \\ h_{19}(x,y,z,s,t) &= \frac{(6\sqrt{rs}\ cosech_v(2\sqrt{-a_1a_3}\xi)\sqrt{-\frac{a_1}{a_3}}\ \lambda a_3)}{\mu\ ln(v)(4a_1a_3-a_2^2)} \\ &\quad + \frac{(6\coth_v(2\sqrt{-a_1a_3}\xi)\sqrt{-\frac{a_1}{a_3}}\lambda a_3 + 4ln(v)\mu a_2^2)}{\mu\ ln(v)(4a_1a_3-a_2^2)}, \\ h_{20}(x,y,z,s,t) &= \frac{\left(3\sqrt{-\frac{a_1}{a_3}}\lambda a_3\right)\left(\tanh_v\left(\frac{1}{2}\sqrt{-a_1a_3}\xi\right)+\coth_v\left(\frac{1}{2}\sqrt{-a_1a_3}\xi\right)\right)}{\mu\ln(v)(4a_1a_3-a_2^2)} \\ &\quad + \frac{\left(4\ln(v)\mu a_1a_3 - \ln(v)\mu {a_2}^2\right)}{\mu\ln(v)(4a_1a_3-a_2^2)}. \end{cases} \tag{12}$$

Case 5: If $a_2 = 0$ *and* $a_3 = a_1$,

$$\begin{cases} h_{21}(x,y,z,s,t) &= \frac{-6a_3\lambda\tan_v(a_1\xi)}{\mu\ln(v)(4a_1a_3-a_2^2)} + 1, \\ h_{22}(x,y,z,s,t) &= \frac{6a_3\lambda\cot(a_1\xi)}{\mu\ln(v)(4a_1a_3-a_2^2)} + 1, \\ h_{23}(x,y,z,s,t) &= \frac{-6\sqrt{rs}\sec_v(2a_1\xi)\lambda a_3 + 4\ln(v)\mu a_1a_3 - \ln(v)\mu {a_2}^2}{\mu\ln(v)(4a_1a_3-a_2^2)} \\ &\quad - \frac{6\tan_v(2a_1\xi)\lambda a_3}{\mu\ln(v)(4a_1a_3-a_2^2)}, \\ h_{24}(x,y,z,s,t) &= \frac{-6\sqrt{rs}\ cosec_v(2a_1\xi)\lambda a_3 + 4\ln(v)\mu a_1a_3 - \ln(v)\mu {a_2}^2}{\mu\ln(v)(4a_1a_3-a_2^2)} \\ &\quad + \frac{6\cot_v(2a_1\xi)\lambda a_3}{\mu\ln(v)(4a_1a_3-a_2^2)}, \\ h_{25}(x,y,z,s,t) &= \frac{-6a_3\lambda\left(\frac{1}{2}\tan_v\left(\frac{1}{2}a_1\xi\right) - \frac{1}{2}\cot_v\left(\frac{1}{2}a_1\xi\right)\right)}{\mu\ln(v)(4a_1a_3-a_2^2)} + 1. \end{cases} \tag{13}$$

Case 6: If $a_2 = 0$ *and* $a_3 = -a_1$,

$$\begin{cases} h_{26}(x,y,z,s,t) &= \frac{6a_3\lambda\ \tanh_v(a_1\xi)}{\mu\ln(v)(4a_1a_3-a_2^2)} + 1, \\ h_{27}(x,y,z,s,t) &= \frac{6a_3\lambda\ \coth_v(a_1\xi)}{\mu\ln(v)(4a_1a_3-a_2^2)} + 1, \\ h_{28}(x,y,z,s,t) &= \frac{-6\sqrt{rs}\sec h_v(2a_1\xi)\iota\lambda a_3 + 4\ln(v)\mu a_1a_3 - \ln(v)\mu {a_2}^2}{\mu\ln(v)(4a_1a_3-a_2^2)} \\ &\quad + \frac{6\tanh_v(2a_1\xi)\lambda a_3}{\mu\ln(v)(4a_1a_3-a_2^2)}, \\ h_{29}(x,y,z,s,t) &= \frac{-6\sqrt{rs}\ cosech_v(2a_1\xi)\lambda a_3 + 4\ln(v)\mu a_1a_3 - \ln(v)\mu {a_2}^2}{\mu\ln(v)(4a_1a_3-a_2^2)} \\ &\quad + \frac{6\cot h_v(2a_1\xi)\lambda a_3}{\mu\ln(v)(4a_1a_3-a_2^2)}, \\ h_{30}(x,y,z,s,t) &= \frac{-6\left(\frac{-1}{2}\tanh_v\left(\frac{1}{2}a_1\xi\right)\frac{-1}{2}\coth_v\left(\frac{1}{2}a_1\xi\right)\right)a_3\lambda}{\mu\ln(v)(4a_1a_3-a_2^2)} + 1. \end{cases} \tag{14}$$

Case 7: If $a_2^2 = 4a_3a_1$,

$$h_{31}(x,y,z,s,t) = \frac{12\,a_3\lambda\,a_1\,(a_2\xi\,\ln(v)+2)}{\mu\,(\ln(v))^2\,(4a_1a_3-a_2^2)\,{a_2}^2\xi} + 1. \tag{15}$$

Case 8: If $a_2 = \lambda, a_1 = p\lambda (p \neq 0)$ *and* $a_3 = 0$,

$$h_{32}(x,y,z,s,t) = \frac{-6\,a_3\lambda\,\left(v^{\lambda\xi} - p\right)}{\mu\,\ln(v)\,(4a_1a_3 - a_2^2)} + 1. \tag{16}$$

Case 9: If $a_2 = a_3 = 0$,

$$h_{33}(x,y,z,s,t) = -\frac{6\,a_3\lambda\,a_1\xi - 4\,\mu\,a_1a_3 + \mu\,{a_2}^2}{\mu\,(4a_1a_3 - a_2^2)}. \tag{17}$$

Case 10: If $a_2 = a_1 = 0$,

$$h_{34}(x,y,z,s,t) = \frac{6\,\lambda}{\mu\,(\ln(v))^2\,(4a_1a_3 - a_2^2)\,\xi} + 1. \tag{18}$$

Case 11: If $a_1 = 0$ *and* $a_2 \neq 0$,

$$\begin{cases} h_{35}(x,y,z,s,t) &= \frac{6\lambda ra_2}{\mu\ln(v)(4a_1a_3-a_2^2)(\cosh_v(\xi a_2) - \sin h(\xi a_2)+r)} + 1, \\ h_{36}(x,y,z,s,t) &= \frac{6\lambda a_2(\sinh(\xi a_2)+\cosh(\xi a_2))}{\mu\ln(v)(4a_1a_3-a_2^2)(\sinh(\xi a_2)+\cosh(\xi a_2)+s)} + 1. \end{cases} \tag{19}$$

Case 12: If $a_2 = \lambda, a_3 = p\lambda$ *and* $a_1 = 0$,

$$h_{37}(x,y,z,s,t) = -\frac{6a_3\lambda v^{\lambda\xi}}{\mu\,ln(v)(4a_1a_3 - a_2^2)(s - prv^{\lambda\xi})} + 1. \tag{20}$$

GRAPHICAL BEHAVIOUR OF WAVE PATTERNS

The main goal of this section is to present the dynamics of the accurate soliton solutions to the BLMP equation. We select values for arbitrary constants and parameters to accurately describe the behavior of the presented solutions. We are able to obtain a variety of well-known and standard Soliton solutions by applying the modified Khater technique to the Boiti Leon Manna Pempinelli equation. These solutions include the solitary wave solutions, sine-functio, cosine-function, tangent-function, cosecant-function, secant-function, cotangent hyperbolic-function, sine hyperbolic-function, secant hyperbolic-function, tangent hyperbolic-function, exponential functions solutions, and a suitable selection of arbitrary constants and parameters that fall within the acceptable range.

We accomplish this by using the symbolic computation tools Mathematica and Matlab. Here is a graphical depiction of the BLMP equation, along with all of the appropriate parametric parameters. Figure 1 illustrates the single-wave behavior of the solution. In the first subfigure (a), we create the three-dimensional

phase plane of the solitary wave solution. In the second subfigure (b), we draw a two-dimensional graph of the solitary wave solution. The third subfigure (c) displays a contour representation of the solitary wave solution. Figure 2 displays the periodic wave solution that we obtained from the Soliton wave equation. We construct the three-dimensional visualization in subfigure (a), we draw the two-dimensional behavior in subfigure (b), and we depict the contour graph in subfigure (c). Figure 3 illustrates the soliton solution's kink behavior for the wave equation. Subfigure (a) displays the 3D visualization, subfigure (b) displays the 2D behavior, and subfigure (c) displays the contour behavior of the solution.

Figure 4 depicts the solution's behavior as a single wave. Subfigure (a) depicts the three-dimensional presentation, whereas subfigure (b) illustrates the two-dimensional visualization, and subsection (c) illustrates the contour behavior of the solution. Figure 5 illustrates the periodic behavior of a soliton solution in relation to the wave equation. Subfigure (a) displays the three-dimensional appearance, subfigure (b) displays the two-dimensional behavior, and subfigure (c) illustrates the contour behavior of the solution.

In addition to these static figures, we uploaded video files visualising the 4D representation of $h_1(x,t,y)$ and $h_6(x,t,y)$ with the rest of the parameters same as in the figure 1 and figure 3. These videos allow us to study the effect of change in one more dimension compared to the static visualisations. The plots for these videos were made using the R statistical software (Team 2020). The files are published in the Zenodo repository. In addition, there are two more videos that contain 2D plots with changes in y (Martinovič et al.2024). These are $h_1(x,y)$ and $h_6(x,y)$ with $t=1$ and the rest of the parameters set as above.

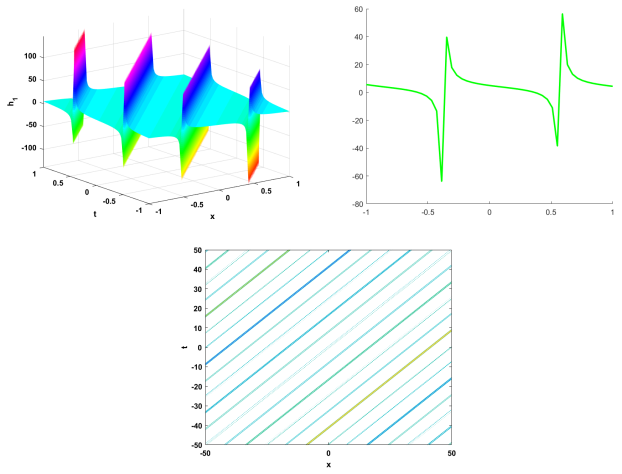

Figure 1 Illustrates solitary wave behavior of the solution for $h_1(x,y,z,s,t)$ with the selected parameter values $k_1=2, k_2=1, k_3=3, k_4=5, a_1=1, a_2=1, a_3=3, \lambda=9, r=1, s_1=2, y=z=s=0$, through 3D, 2D and contour graphs in the suitable ranges.

PHASE PORTRAIT ANALYSIS

In this section of the article, we will use bifurcation analysis to investigate Eq.1. We can use a Galilean transformation to convert Eq.5 into a set of ordinary differential equations, as follows by letting $f^{'}=h$.

$$\delta_0 h+\delta_1 h^{''}+\delta_2 h^2=0 \tag{21}$$

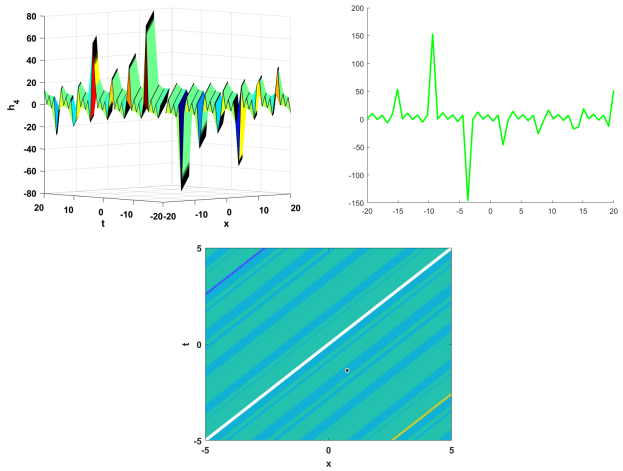

Figure 2 Shows periodic soliton solution for $h_4(x,y,z,s,t)$ with the parameters values $k_1=2, k_2=1, k_3=3, k_4=5, a_1=1, a_2=1, a_3=3, \lambda=9, r=1, s_1=2, y=z=s=0$, by utilizing 3D, 2D and contour graphs respectively in suitable boundary values.

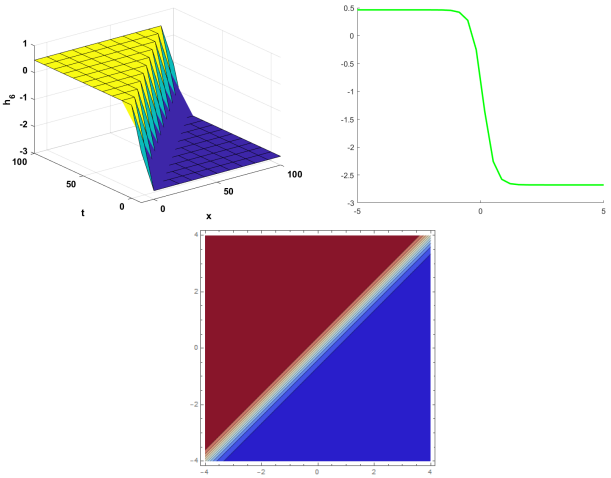

Figure 3 Displays combined dark and bright cubic soliton solution for $h_6(x,y,z,s,t)$ with the help of suitable parameters value $k_1=2, k_2=1, k_3=3, k_4=5, a_1=1, a_2=3, a_3=1, \lambda=9, r=1, s_1=2, y=z=s=0$, through 3D, 2D and contour graphs with appropriate boundary.

Let $h^{'}=y$ and $h^{''}=y^{'}$, so, we finally have Planner dynamical system as:

$$\begin{cases} \frac{dh}{d\xi}=y, \\ \frac{dy}{d\xi}=\sigma_1 h-\sigma_2 h^2 \end{cases} \tag{22}$$

Where, $\sigma_1=-\frac{\delta_0}{\delta_1}$ and $\sigma_2=-\frac{\delta_2}{\delta_1}$. This system expresses Hamiltonian features and possesses the following integral:

$$G(h,y)=\frac{y^2}{2}-\frac{\sigma_1 h^2}{2}+\frac{\sigma_2 h^3}{3}=g. \tag{23}$$

Where, g is a Hamiltonian constant, we analyze the equilibrium points of the phase portraits within the parameter defined by σ_1

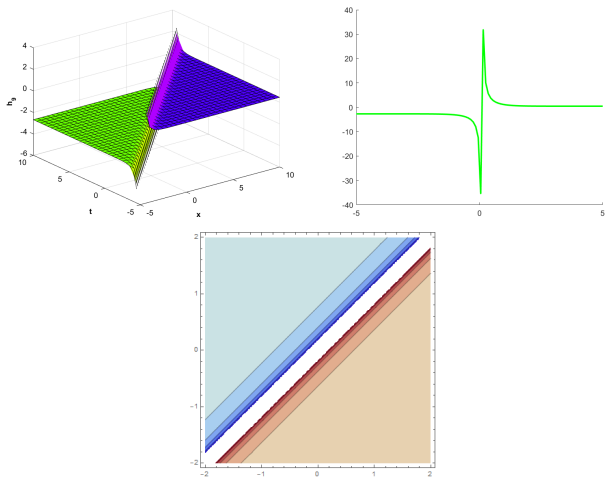

Figure 4 Shows rational soliton solution for $h_9(x, y, z, s, t)$ with the suitable parameters $k_1 = 2, k_2 = 1, k_3 = 3, k_4 = 4, a_1 = 1, a_2 = 3, a_3 = 1, \lambda = 9, r = 1, s_1 = 2, y = z = s = 0$, by 3D, 2D and contour graphs in the proper range.

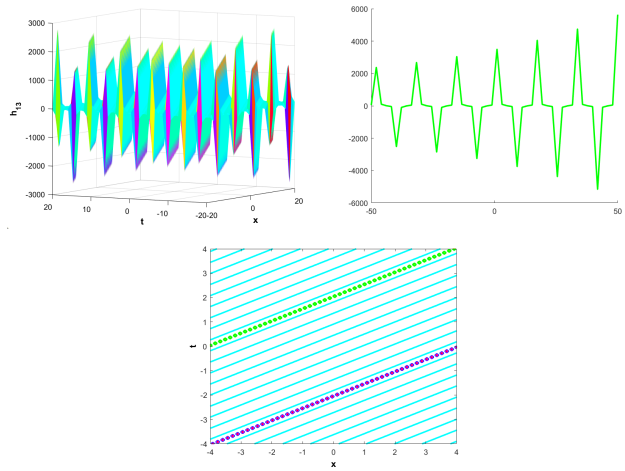

Figure 5 Presents periodic soliton solution for $h_{13}(x, y, z, s, t)$ with the suitable parameters values $k_1 = 2, k_2 = 1, k_3 = 3, k_4 = 4, a_1 = 1, a_2 = 0, a_3 = 1, \lambda = 9, r = 1, s_1 = 2, y = z = s = 0$, through 3D, 2D and contour graphs in proper range.

and σ_2 for the system. By utilizing qualitative analysis, the two equilibrium points for the differential equation system described above are $M_1(\frac{\sigma_1}{\sigma_2}, 0)$ and $M_2(0, 0)$. Therefore, the Jacobian of the system will be:

$$det(J(h,y)) = \begin{vmatrix} 0 & 1 \\ \sigma_1 - 2\sigma_2 h & 0 \end{vmatrix} = 2\sigma_2 h - \sigma_1. \tag{24}$$

Thus, the point (h, y) is a centre point for the det $J(h, y) > 0$, it is a saddle for the det $J(h, y) < 0$, and it is a cuspidal point for the det $J(h, y) = 0$. By assigning different values to the parameters that are involved, it is possible to get a wide variety of results.

Case 1: For $\sigma_1 > 0$ and $\sigma_2 > 0$, we get two equilibrium points by using $\delta_0 = -4, \delta_1 = -2$, and $\delta_2 = -6$. These values allow us to obtain $M_1 = (\frac{2}{3}, 0)$ and $M_2 = (0, 0)$. In Figure 6(a), the term M_1, representing the center point, denotes the equilibrium point, while the term M_2 represents the saddle point.

Case 2: Using the values $\delta_0 = 4, \delta_1 = 2$, and $\delta_2 = 6$, we have two equilibrium points $M_1 = (\frac{2}{3}, 0)$, and M_2= (0, 0) for $\sigma_1 < 0$ and $\sigma_2 < 0$. M_1 is the saddle point, and M_2 is the center point, as shown to Fig. 6(b).

Case 3: With $\sigma_1 > 0$ and $\sigma_2 < 0$, it is possible to get two equilibrium points by applying $\delta_0 = -4, \delta_1 = 2$, and $\delta_2 = -6$. These two equilibrium points are denoted as $M_1 = (-\frac{2}{3}, 0)$ and $M_2 = (0, 0)$ respectively. The point M_1 represents the center of the curve, and the point M_2 represents the saddle point in Figure 6(c).

Case 4: For $\sigma_1 < 0$ and $\sigma_2 > 0$, using $\delta_0 = 4, \delta_1 = 2$ *and* $\delta_2 = -6$ there are two equilibrium points obtained. $M_1 = (-\frac{2}{3}, 0)$ and $M_2 = (0, 0)$. M_1 denotes the saddle point and M_2 shows the centre point in Fig.6(d).

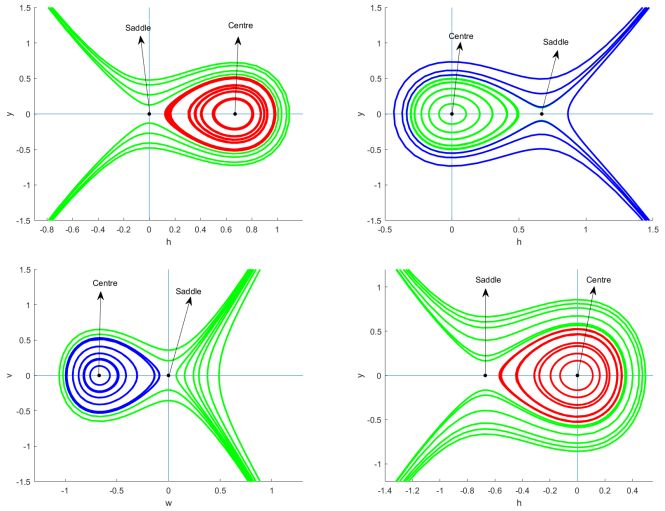

Figure 6 Phase portrait of system (22), Fig. 6(a) for $\sigma_1 > 0$ and $\sigma_2 > 0$, Fig. 6(b) for $\sigma_1 < 0$ and $\sigma_2 < 0$., Fig. 6(c) for $\sigma_1 < 0$ and $\sigma_2 < 0$., and Fig. 6(d) for $\sigma_1 < 0$ and $\sigma_2 > 0$ respectively.

CHAOTIC BEHAVIOR

In this part, we will examine the chaotic patterns exhibit by the model that is under study. We propose to add an external force $\theta_0 \cos(\Lambda\xi)$ to the system in order to investigate these patterns (22). The amplitude of this perturbed term is θ_0, and its frequency is Λ. As a result, the transformed system has the following expression:

$$\begin{cases} \frac{dh}{d\xi} = y \\ \frac{dy}{d\xi} = \sigma_1 h + \sigma_2 h^2 + \theta_0 \cos(\mathcal{F}), \\ \frac{d\mathcal{F}}{d\xi} = \Lambda, \end{cases} \tag{25}$$

where $\mathcal{F} = \Lambda\xi$. The system's quasi-periodic and chaotic features have been investigated (25) using numerous kinds of techniques, such as time plots and phase plots in 2D and 3D dimensions. In order to identify the dynamical behaviors of the disturbed system, a range of random values for physical parameters are examined. Keeping the other parameters constant at $\sigma_1 = -3.5$ and $\sigma_2 = -1$, we will investigate the effects of changing both θ_0 and Λ.

• Phase plots and time series graphs for $\theta_0 = 0.6$ and $\Lambda = 0.5$ are shown in Figure (7). Here, the system (25) exhibits periodic behavior since the external force's frequency and intensity are both very low.
• The 3D plot, 2D plot, and time analysis graph are shown in Figure (8) as the intensity is increased with $\theta_0 = 1.6$ and frequency with $\Lambda = 2.5$. It has been noted that the altered disturbed system (25) exhibits quasi-periodic behavior.
• We show both 2D and 3D phase images in Figure (9), together with time analysis for the following parameter values: $\theta_0 = 3.6$ and $\Lambda = 2\pi$. According to the reported results, it can be concluded that changes in these parameters cause the system to exhibit a quasi-periodic chaotic pattern (25).
• The investigation of the amplitude and frequency varies when $\theta_0 = 5.6$ and $\Lambda = 2\pi$, as shown in Figure (10). The final results show that chaotic events are present in the modified system.

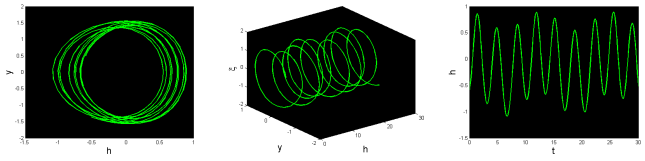

Figure 7 Detection of chaotic phenomena in the perturbed system (25), $\theta_0 = 0.6$.

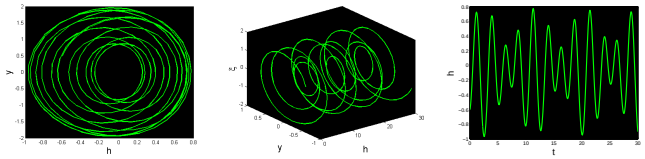

Figure 8 Detection of chaotic phenomena in the perturbed system (25), $\theta_0 = 1.6$.

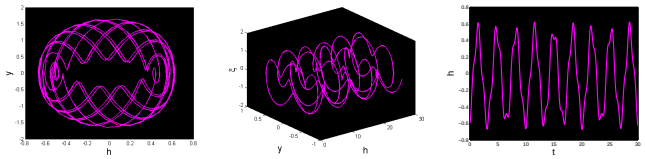

Figure 9 Detection of chaotic phenomena in the perturbed system (25), $\theta_0 = 3.6$.

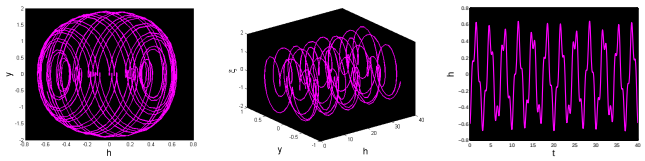

Figure 10 Detection of chaotic phenomena in the perturbed system (25), $\theta_0 = 5.6$.

Sensitivity Analysis

Here, we examine the system's sensitivity to the perturbation system (25). To achieve this goal, we took into account three different initial conditions: The green solid line illustrates $(h, y) = (0.02, 0.5)$, the blue dotted curve illustrates $(h, y) = (0.05, 1)$, and the red dashed curve illustrates $(h, y) = (1.2, 1.2)$. Figure (11) considers the values of the parameters $(h, y) = (0.02, 0.5)$ and $(h, y) = (0.05, 1)$ to address two different solutions. While one of these solution aims to get green, the other one aims to achieve blue. In addition, Figure 12 presents two more solutions, namely $(h, y) = (0.02, 0.5)$ and $(h, y) = (1.2, 1.2)$. One of these solutions pertains to green, while the other pertains to blue. Additionally, in Figure (13), two additional solutions are employed. These solutions are as follows: $(h, y) = (0.05, 1)$ and $(h, y) = (1.2, 1.2)$. The three solutions that are combined are shown in Figure (14) as the green, blue, and red lines, respectively, as $(0.02, 0.5)$, $(0.05, 1)$, and $(1.2, 1.2)$. In a dynamic system, it is evident that even little changes in the initial conditions may result in subtle adjustments in the results the system provides. As a result, we are able to draw the conclusion that the proposed system is sensitive, but not to an extremely high degree.

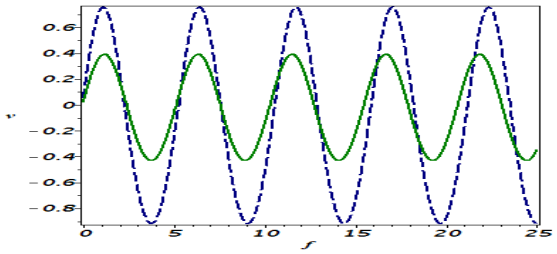

Figure 11 Sensitivity analysis of the system (25), $(h, y) = (0.02, 0.5)$ and $(h, y) = (0.05, 1)$.

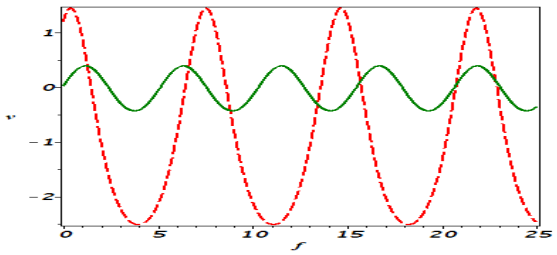

Figure 12 Sensitivity analysis of the system (25), $(h, y) = (0.02, 0.5)$ and $(h, y) = (1.2, 1.2)$.

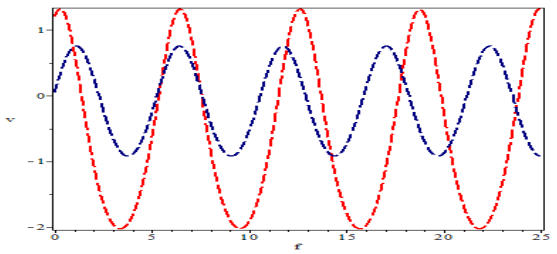

Figure 13 Sensitivity analysis of the system (25), $(h, y) = (0.05, 1)$ and $(h, y) = (1.2, 1.2)$.

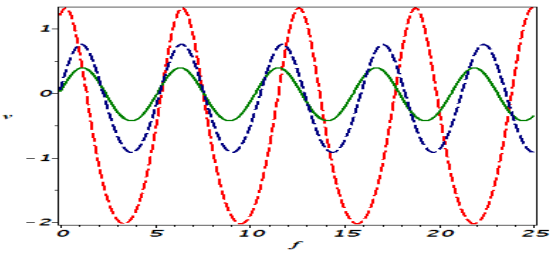

Figure 14 Sensitivity analysis of the system (25), $(0.02, 0.5)$, $(0.05, 1)$, and $(1.2, 1.2)$.

CONCLUSION

This work is unique because it generates soliton wave solutions to the Boiti Leon Manna Pempinelli equation, which is a four-dimensional equation. We use a modified version of the Khater technique to compute the precise solutions to the solitary wave equation. We have confirmed the correctness of our offered solutions through the use and verification of numerous graphs. The obtained solutions take various shapes, including trigonometric, rational expressions and hyperbolic. We have explored a wide range of parameter values for the established ordinary differential equations, methodically generating a variety of soliton profiles.

We constructed 3D, 2D, and contour diagrams, as well as a 4D visualization, by using the software programs Matlab, Mathematica, and R-language, with the parameter values carefully set. We generate these graphs to underscore the physical importance of the proposed model. These graphical and video representations are significant because they reveal our research's findings. In order to have a more profound understanding of the dynamical behavior of the governing system, the phase-portrait system and chaos theories are used. The graphs in figures illustrate the process by which the chaotic solutions to the perturbed dynamical system are discovered and shown in figures (7-10). Investigations into the model's sensitivity reveal that it is extremely sensitive, as shown in figures (11–14). Based on the findings, it is clear that the suggested methods are efficient tools for analyzing nonlinear evolution equations, and that they provide valuable insights into the model.

Acknowledgments

This article has been produced with the financial support of the European Union under the REFRESH – Research Excellence For Region Sustainability and High-tech Industries project number CZ.10.03.01/00/22_003/0000048 via the Operational Programme Just Transition.

Availability of data and material

All data that support the findings of this study are included within the article.

Conflicts of interest

The authors declare that there is no conflict of interest regarding the publication of this paper.

Ethical standard

The authors have no relevant financial or non-financial interests to disclose.

LITERATURE CITED

Akinyemi, L., H. Rezazadeh, S.-W. Yao, M. A. Akbar, M. M. Khater, *et al.*, 2021 Nonlinear dispersion in parabolic law medium and its optical solitons. Results in Physics **26**: 104411.

Al-Smadi, M., 2018 Simplified iterative reproducing kernel method for handling time-fractional bvps with error estimation. Ain Shams Engineering Journal **9**: 2517–2525.

Al-Smadi, M., O. A. Arqub, and D. Zeidan, 2021 Fuzzy fractional differential equations under the mittag-leffler kernel differential operator of the abc approach: Theorems and applications. Chaos, Solitons & Fractals **146**: 110891.

Bibi, S., S. T. Mohyud-Din, U. Khan, and N. Ahmed, 2017 Khater method for nonlinear sharma tasso-olever (sto) equation of fractional order. Results in physics **7**: 4440–4450.

Biswas, A., M. Mirzazadeh, M. Eslami, Q. Zhou, A. Bhrawy, *et al.*, 2016 Optical solitons in nano-fibers with spatio-temporal dispersion by trial solution method. Optik **127**: 7250–7257.

Conte, R. and M. Musette, 1992 Link between solitary waves and projective riccati equations. Journal of Physics A: Mathematical and General **25**: 5609.

Feng, Z., 2002 The first-integral method to study the burgers–korteweg–de vries equation. Journal of Physics A: Mathematical and General **35**: 343.

Fokas, A., 2016 Integrable multidimensional versions of the nonlocal nonlinear schrödinger equation. Nonlinearity **29**: 319.

He, J.-H. and L.-N. Zhang, 2008 Generalized solitary solution and compacton-like solution of the jaulent–miodek equations using the exp-function method. Physics Letters A **372**: 1044–1047.

Jamal, T., A. Jhangeer, and M. Z. Hussain, 2023 Analysis of nonlinear dynamics of novikov–veselov equation using solitonic solutions, bifurcation, periodic and quasi-periodic solutions, and poincaré section. The European Physical Journal Plus **138**: 1087.

Khater, M., S. Anwar, K. U. Tariq, and M. S. Mohamed, 2021a Some optical soliton solutions to the perturbed nonlinear schrödinger equation by modified khater method. AIP Advances **11**.

Khater, M., S. Anwar, K. U. Tariq, and M. S. Mohamed, 2021b Some optical soliton solutions to the perturbed nonlinear schrödinger equation by modified khater method. AIP Advances **11**.

Khater, M., R. A. Attia, and D. Lu, 2021c Superabundant novel solutions of the long waves mathematical modeling in shallow water with power-law nonlinearity in ocean beaches via three recent analytical schemes. The European Physical Journal Plus **136**: 1–19.

Khater, M. M., 2021a Abundant breather and semi-analytical investigation: On high-frequency waves' dynamics in the relaxation medium. Modern Physics Letters B **35**: 2150372.

Khater, M. M., 2021b Diverse solitary and jacobian solutions in a continually laminated fluid with respect to shear flows through the ostrovsky equation. Modern Physics Letters B **35**: 2150220.

Khater, M. M., A. R. Seadawy, and D. Lu, 2017 Elliptic and solitary wave solutions for bogoyavlenskii equations system, couple boiti-leon-pempinelli equations system and time-fractional cahn-allen equation. Results in physics **7**: 2325–2333.

Kim, H., J.-H. Bae, and R. Sakthivel, 2014 Exact travelling wave solutions of two important nonlinear partial differential equations. Zeitschrift für Naturforschung A **69**: 155–162.

Kruglov, V. I. and H. Triki, 2021 Periodic and solitary waves in an inhomogeneous optical waveguide with third-order dispersion and self-steepening nonlinearity. Physical Review A **103**: 013521.

Kudryashov, N., 1991 On types of nonlinear nonintegrable equations with exact solutions. Physics Letters A **155**: 269–275.

Lee, J., R. Sakthivel, and L. Wazzan, 2010 Exact traveling wave solutions of a higher-dimensional nonlinear evolution equation. Modern Physics Letters B **24**: 1011–1021.

Li, Y., W.-r. Shan, T. Shuai, and K. Rao, 2015 Bifurcation analysis and solutions of a higher-order nonlinear schrödinger equation. Mathematical Problems in Engineering **2015**: 408586.

Liu, H., H. Yang, N. Liu, and L. Yang, 2022 Bifurcation and chaos analysis of tumor growth. International Journal of Biomathematics **15**: 2250039.

Liu, S., Z. Fu, S. Liu, and Q. Zhao, 2001 Jacobi elliptic function expansion method and periodic wave solutions of nonlinear wave equations. Physics Letters A **289**: 69–74.

Ma, W.-x., 1993 Travelling wave solutions to a seventh order generalized kdv equation. Physics Letters A **180**: 221–224.

Nikan, O., S. M. Molavi-Arabshai, and H. Jafari, 2021 Numerical simulation of the nonlinear fractional regularized long-wave model arising in ion acoustic plasma waves. Discret. Contin. Dyn. Syst. S **14**: 3685–3701.

Özer, A. and E. Akın, 2005 Tools for detecting chaos. Sakarya University Journal of Science **9**: 60–66.

Park, C., M. M. Khater, A.-H. Abdel-Aty, R. A. Attia, H. Rezazadeh, *et al.*, 2020 Dynamical analysis of the nonlinear complex fractional emerging telecommunication model with higher–order dispersive cubic–quintic. Alexandria Engineering Journal **59**: 1425–1433.

Raza, N., A. Jhangeer, S. Arshed, and M. Inc, 2024 The chaotic, supernonlinear, periodic, quasiperiodic wave solutions and solitons with cascaded system. Waves in random and complex media **34**: 1726–1740.

Raza, N., M. Kaplan, A. Javid, and M. Inc, 2022 Complexiton and resonant multi-solitons of a (4+ 1)-dimensional boiti–leon–manna–pempinelli equation. Optical and Quantum Electronics **54**: 1–16.

Saha, A., 2017 Bifurcation, periodic and chaotic motions of the modified equal width-burgers (mew-burgers) equation with external periodic perturbation. Nonlinear Dynamics **87**: 2193–2201.

Sheng, Z., 2006 The periodic wave solutions for the (2+ 1)-dimensional konopelchenko–dubrovsky equations. Chaos, Solitons & Fractals **30**: 1213–1220.

Singh, J., D. Kumar, Z. Hammouch, and A. Atangana, 2018 A fractional epidemiological model for computer viruses pertaining to a new fractional derivative. Applied mathematics and computation **316**: 504–515.

Tchaho, C. T. D., H. M. Omanda, G. N. Mbourou, J. R. Bogning, and T. C. Kofané, 2021 Higher order solitary wave solutions of the standard kdv equations. Open Journal of Applied Sciences **11**: 103–125.

Team, R. C., 2020 Ra language and environment for statistical computing, r foundation for statistical. Computing .

Valdés, J. E. Ñ., 2003 La resolución de problemas en la enseñanza de las ecuaciones diferenciales ordinarias. un enfoque histórico. Revista Educación y Pedagogía pp. 163–181.

Wang, D.-S., 2009 A systematic method to construct hirota's transformations of continuous soliton equations and its applications. Computers & Mathematics with Applications **58**: 146–153.

Wazwaz, A.-M., 2004 A sine-cosine method for handlingnonlinear wave equations. Mathematical and Computer modelling **40**: 499–508.

Wazwaz, A.-M., 2007 Traveling wave solution to (2+ 1)-dimensional nonlinear evolution equations. J. Nat. Sci. Math **1**: 1–13.

Wu, Z., W. Zhang, and X. Zeng, 2023 Exploring the short-term and long-term linkages between carbon price and influence factors considering covid-19 impact. Environmental Science and Pollution Research **30**: 61479–61495.

Xu, G.-Q. and X.-Z. Huang, 2013 New variable separation solutions for two nonlinear evolution equations in higher dimensions. Chinese Physics Letters **30**: 030202.

Xu, G.-Q. and A.-M. Wazwaz, 2019 Integrability aspects and localized wave solutions for a new (4+ 1)-dimensional boiti–leon–manna–pempinelli equation. Nonlinear Dynamics **98**: 1379–1390.

Zheng-Zheng, Y. and Y. Zhen-Ya, 2009 Symmetry groups and exact solutions of new (4+ 1)-dimensional fokas equation. Communications in Theoretical Physics **51**: 876.

How to cite this article: Iqbal, M., Riaz, M. B., Rehman, M. A., Martinovic, T. and Martinovic, J. Demonstration of Sensitive Analysis and Optical Soliton Patterns in a (4+1) Dimensional Boiti-Leon-Manna Pempinelli Equation: Dynamic Insights into Bifurcation, Chaotic Behavior. *Chaos Theory and Applications*, 7(1), 1-9, 2025.